

**BIOCHEMICAL CHARACTERIZATION OF ISOFORM-
SPECIFIC INHIBITORS OF ACYL PROTEIN THIOESTERASE
ENZYMES**

Sin Ye Hwang

04/18/2015

This thesis has been read and approved by Dr. Brent Martin.

Signed:

Date: ____ / ____ / ____

Faculty advisor email: brentrm@umich.edu

Phone:

Table of Contents

Abstract.....	1
Introduction.....	2
Materials and Methods.....	5
Results and Discussion.....	10
1. Characterizing APT1 & 2 Mutants: Selectivity determinants.....	10
2. Characterizing ML349 inhibitor derivatives: What defines the active site?.....	15
Acknowledgements.....	23
References.....	25

Abstract

Protein palmitoylation plays an important role in the function, trafficking and localization of many membrane-associated proteins, including the oncogenic Ras proteins^{1,2}. Acyl protein thioesterase (APT) enzymes – APT1 and APT2 – are homologous enzymes (68% identity) that are thought to catalyze depalmitoylation of proteins involved in key cellular processes. Although, very little is known about their substrate specificities or regulation, recent studies have discovered two small molecule inhibitors – ML348 and ML349 – that are selective towards APT1 and APT2 respectively³. We hypothesized that by switching certain key residues between APT1 and APT2, we will be able to reverse the ligand selectivity of the two isoforms. Thus, we characterized the kinetics of the APT mutants with isoform-specific inhibitors, and identified key residues, Ile75 in APT1 and Pro86 in APT2, in a loop region that likely plays an important role in switching ligand and probably endogenous substrate specificity. We have also synthesized and characterized APT2 inhibitor derivatives to find better inhibitors of APT enzymes, which can help elucidate the environment of the substrate-binding pocket. Future directions of this project include utilizing APT isoform-selective inhibitors to identify the native substrates of APT enzymes in order to understand their role in regulation.

Introduction

Protein S-palmitoylation is the dynamic, post-translational modification in which fatty acids are added to proteins through reversible cysteine thioester linkages. The addition of this hydrophobic moiety helps anchor soluble proteins to cell membranes and endomembranes such as the endoplasmic reticulum (ER) and Golgi membranes. Therefore, palmitoylation plays critical roles in the function, trafficking and localization of various peripheral membrane proteins^{4,5}.

The reversibility of this process involves cycles of fatty acid addition by DHHC protein acyltransferases (PATs) and fatty acid hydrolysis by depalmitoylating enzymes such as acyl-protein thioesterases (APT).

The PATs involved in this process are characterized by the DHHC catalytic motif, which is named after the conserved catalytic Asp-His-His-Cys sequence located in a cysteine-rich region. The catalytic mechanism involves first, autoacylation at the DHHC cysteine using an acyl-CoA donor, and then the transfer of the fatty acid onto the substrate protein⁶. To date, 23 DHHC proteins have been identified in humans, suggesting divergence in substrate specificity, activity or regulation⁷. This is supported by the observation that sequence conservation in PATs is limited to the 51-amino acid DHHC domain, whereas the

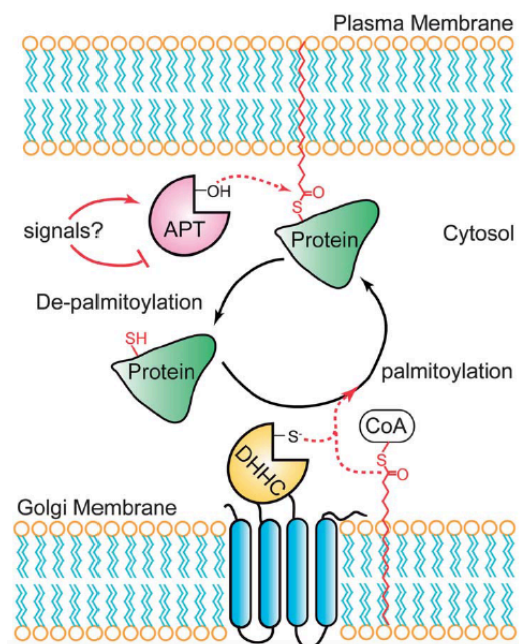


Figure 1: Dynamic S-palmitoylation cycles of certain palmitoylated proteins between the plasma membrane and endomembranes such as the Golgi. Thioesterases hydrolyze the fatty acid chain from the protein, thus abrogating the association of the protein to the membrane. The protein dissociates into the cytosol, but can be re-palmitoylated by DHHC palmitoyl transferases in the Golgi, thus allowing the protein to be recycled back to the membrane.

amino- and carboxy-terminal domains are more variable and are proposed to contain domains determining protein-protein interactions and substrate binding⁵.

In contrast, very few proteins have been conclusively identified as depalmitoylating enzymes, two of which are the acyl-protein thioesterases APT1 and APT2. In some of the literature, APT1 and APT2 are also identified as lysophospholipases LYPLA1 and LYPLA2 as they were first discovered due to their ability to hydrolyze various lysophospholipids⁸. However, they were later shown to have much higher affinity and hydrolytic efficiency against acylated proteins, and were thus renamed acyl-protein thioesterases⁹. APT1 and APT2 belong to the alpha/beta serine hydrolase family, containing the conserved Ser-His-Asp catalytic triad, in which the catalytic serine acts as a nucleophile to covalently attack the thioester linkage of the acyl-protein substrate, forming a transient covalent acyl-intermediate with the fatty acid to be removed¹⁰.

Although over 400 palmitoylated proteins have been annotated in humans through proteomic studies^{11,12}, most of these palmitoylated proteins are relatively stable, suggesting that dynamic palmitoylation is not a general phenomenon, but rather specific to certain regulatory pathways¹¹. Several of these pathways are implicated in various cancers, thus making dynamic palmitoylation an attractive area of research for potential therapies. For instance, the oncogenic GTPases H-Ras and N-Ras require attachment to the cell membrane to induce cell transformation, and both undergo cycles of palmitoylation and depalmitoylation that dictates their localization between the plasma membrane, and ER and Golgi membranes depending on their palmitoylation states². Importantly, these pathways are likely regulated through different means, since H-Ras subcellular localization is affected by APT1 overexpression, whereas N-Ras subcellular localization is not¹, thus highlighting the importance of developing methods to

selectively study specific palmitoylating or depalmitoylating enzymes to establish their specific signaling pathways.

Although APT1 and APT2 are both very similar proteins (68% sequence identity), these two enzymes are likely to have non-redundant functions. For instance, growth-associated protein-43 (GAP-43) is deacylated by APT2 but not APT1¹³, whereas calcium-activated potassium (BK) channels are deacylated by APT1 but not APT2¹⁴. Thus, the development of isoform-selective inhibitors is necessary in order to isolate the specific downstream targets of APT1 and APT2. A previous high-throughput screen of APT1 and APT2 against a NIH library of 315,004 compounds yielded two promising isoform-selective inhibitors - ML348 and ML349 - for APT1 and APT2 respectively³. These compounds are potentially useful tools to probe the specificities of APT1 and APT2. In this thesis project, we used these compounds to probe the selectivities of point mutants of APT1 and APT2 to identify structures in the active site that confer substrate selectivity. We then synthesized and characterized various derivatives of ML349 to further probe the active site of APT2. We hope that these results will lay the foundation for future studies characterizing the substrate specificities of APT1 and APT2, in the hopes of developing better inhibitors.

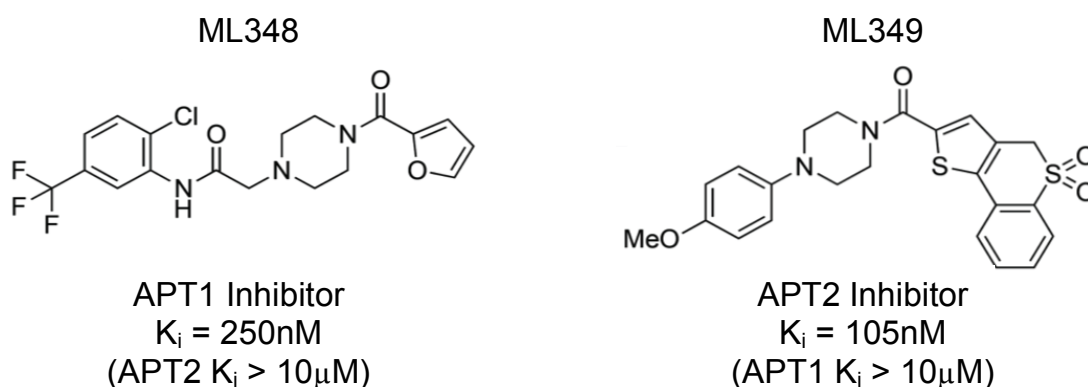


Figure 2: Structures of the APT1-selective inhibitor (ML348) and APT2-selective inhibitor (ML349) and their K_i values for APT1 and APT2.

Materials and Methods

1. Bacterial transformation and protein purification

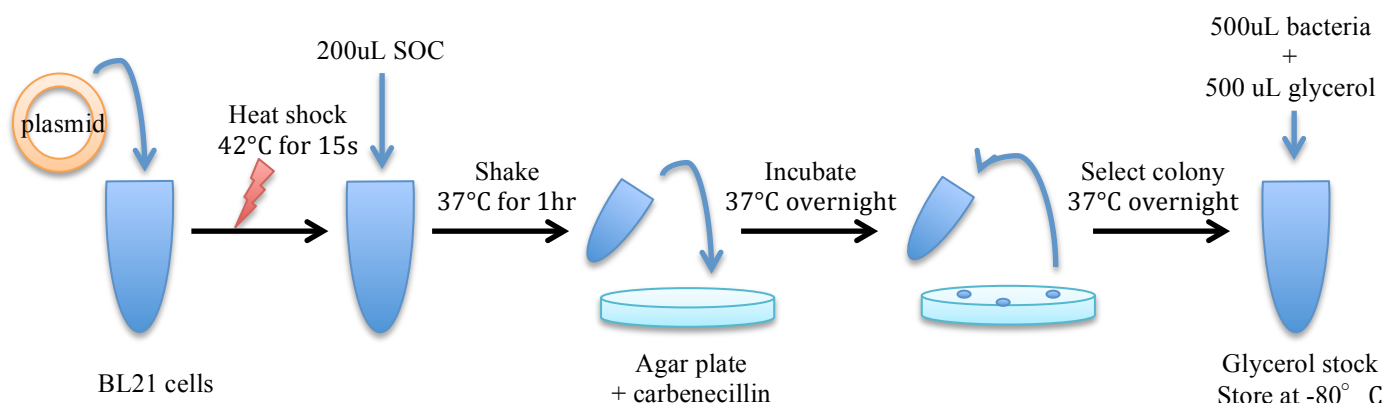


Figure 3: Pictorial depiction of the procedure for bacterial transformation and creation of glycerol stocks for all APT1 and APT2 variants.

BL21 chemically competent cells were incubated with 2 µL of plasmid DNA containing the gene of interest for 30 min on ice. Heat shock was applied at 42°C for 15 seconds, and then cooled on ice for 5 min. 200 µL of SOC media was added, and the mixture was then shaken for 60 min at 37°C. The cells were then plated onto an agar plate containing carbenecillin to select for successfully incorporated plasmids, incubated upside down overnight at 37°C, and subsequently stored at 4°C. A single colony was then selected from the agar plate and grown overnight in 5 mL of TB media (13.3g/L yeast extract, 26.7g/L tryptone, 4.4ml/L glycerol) in a mini culture tube at 37°C while shaking continuously. 500 µL of the mini culture was then added to 500 µL of 100% glycerol and stored at -80°C for use as glycerol stocks.

Protein growth was initiated by selecting cells from glycerol stocks and growing them at 37°C, first in a 10 mL miniculture overnight, and then in 1L TB media, while shaking continuously. Once an optical density of 0.5 at 600nm was achieved, protein expression was induced by addition of 1mM IPTG and the cells were allowed to grow for overnight at room temperature while shaking continuously.

Cells were harvested by centrifugation at 5,000g for 5 min. The pellets were then resuspended in lysis buffer (150mM NaCl, 10% glycerol, 50mM HEPES, pH 7.5) and sonicated at 4°C. The resultant cell debris was further centrifuged at 12,000g for 30 min. The supernatant was mixed with cobalt resin, rotated end over end on at 4°C for 15 min and centrifuged at 2,000 rpm for 4 min. The resin-containing pellet was washed 3 times in wash buffer (150mM NaCl, 50mM HEPES, 1mM imidazole, pH 7.5), and the His-tagged protein of interest was eluted 6 times with elution buffer (150mM NaCl, 50mM HEPES, 50mM imidazole, pH 7.5). Elution fractions containing the overexpressed protein were identified using the DC Protein Assay (Bio-Rad), pooled together and dialyzed 3 times in 1L dialysis buffer (elution buffer minus imidazole) at 4°C. Protein concentration was then determined using the DC Protein Assay, and protein was stored in 25% glycerol at -80°C.

2. Steady-state resorufin acetate hydrolysis assay

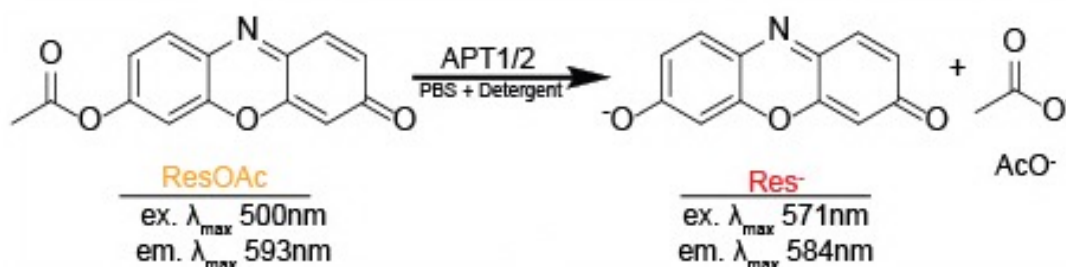


Figure 4: The molecular structures of resorufin acetate and its hydrolyzed form as catalyzed by APT1 and 2 is shown, along with the fluorescence excitation and emission wavelengths of each structure.

Resorufin acetate (ResOAc) was used as a substrate analog to measure the steady state reaction velocities of APT1 and APT2. The acetyl group of ResOAc is hydrolyzed by APTs, producing the fluorescent Res⁻ product which has distinct fluorescent properties compared to substrate ResOAc that we can measure using a Tecan F500 microplate reader equipped with excitation and emission filters $\lambda_{\text{ex}} = 535(25)\text{nm}$, $\lambda_{\text{em}} = 590(20)\text{nm}$ respectively. Thus, the catalytic rate of APTs can be assayed by measuring

the rate of production of fluorescent Res⁻ over time. In order to account for spontaneous hydrolysis of ResOAc by water or non-active site residues of APTs, WT APT1 and 2 were assayed alongside catalytic dead mutants APT1-S119A or APT2-S122A respectively.

Measuring substrate dependence (K_m): Reaction buffer was prepared using 1X PBS with 0.01% pluronic adjusted to pH 6.5 using HCl. ResOAc was diluted with DMSO to various 20X concentrations ranging from 1.18 μM to 140 μM. Active and catalytic dead enzymes were diluted with reaction buffer to 10.526 nM. The reaction was initiated by adding 95 μL of 10.526 nM enzyme to 5 μL of 20X ResOAc of various concentrations in a clear, flat-bottomed, 96 well plate (Final concentration: 10nM enzyme, 5% DMSO, 1X ResOAc). Fluorescence intensity was then measured using a TECAN infinite f500 microplate reader at regular time intervals ($\lambda_{\text{ex}} = 535(25)\text{nm}$, $\lambda_{\text{em}} = 590(20)\text{nm}$). At least 4 technical replicates and 2 biological replicates were performed for each concentration of ResOAc. Fluorescence intensities from the catalytic dead enzymes were subtracted from that of the active enzyme to account for background fluorescence. Adjusted fluorescence intensity was then plotted against time and averaged across replicates to obtain v_0 (initial rate of reaction) from the slope of the linear portion of the curves. v_0 was then plotted against [ResOAc] and fitted to the Michaelis-Menton equation, as shown in Equation 1, using Prism or the solver function in Excel to obtain the K_m.

$$v_0 = \frac{V_{\text{max}}[S]}{K_m + [S]} \quad \text{Equation 1}$$

Measuring inhibitor dose-response (IC₅₀ and K_i): Reaction buffer was prepared as described in the substrate dependence assay above. Inhibitors were diluted with DMSO to various concentrations at 48.421X final concentration. Active and catalytic dead enzymes were diluted to 10.76nM concentration using reaction buffer. For each

inhibitor concentration, 10uL of inhibitor was incubated with 450uL of 10.76nM enzyme for 30 minutes. The reaction was initiated by adding 95uL of the enzyme-inhibitor mix to 5uL of 1mM ResOAc in a clear, flat-bottomed, 96-well plate (Final concentration: 10nM enzyme, 7.06% DMSO, 50uM ResOAc, 1X inhibitor). 4 technical replicates and 2 biological replicates were performed for each concentration of inhibitor. Fluorescence intensity and v_0 was obtained as described in the substrate-dependence assay above. v_0 was then plotted against inhibitor concentration and fitted to the four parameter logistic equation (Equation 2) shown below using Prism or the solver function in Excel to obtain the IC_{50} . K_i was then calculated using the Cheng-Prusoff equation (Equation 3)¹⁵.

$$v_i^{res}(I) = \lim_{[I] \rightarrow \infty} v_i^{res} + \frac{\text{Span}}{1 + 10^{(\log IC_{50} - [I]) \times \text{Hill}}} \quad \text{Equation 2}$$

$$K_i = \frac{IC_{50}}{1 + \frac{[S]}{K_m}} \quad \text{Equation 3}$$

3. Thermal shift assay

Protein and dye concentrations for the ThermoFluor assay were first optimized for APT1 and APT2, and determined to be 0.2mg/mL protein and 0.2mM Anilinoanthracene-9-sulfonic acid (1,8-ANS) [AnaSpec AS-81525]. Inhibitors to be tested were dissolved in 100% DMSO to create differing stock concentrations (5.00mM, 3.33mM, 2.22mM, 1.48mM, 0.99mM, 0mM).

For the assay, master mixes were created by adding 1.5uL of stock inhibitors to 1uL of 10mM 1,8-ANS and 47.5uL of 0.2105mg/mL protein in 1X PBS (Final concentrations: [I]=0-150uM, [1,8-ANS]=0.2mM, [protein]=0.2mg/mL, [DMSO]=5%). 10uL of each master mix was aliquot into a 384-well plate [Axygen PCR-384-55-BK] with 4 replicates. 3.2uL of silicone oil [Aldrich 378321] was added to prevent evaporation. The plate was centrifuged at 1000rpm for 1 min. The thermal shift measurements were then performed using a ThermoFluor instrument (Johnson &

Johnson Pharmaceutical Research and Development, L.L.C) using continuous ramping mode from 25°C to 90°C in increments of 1°C, holding 1 minute at each temperature.

Data was analyzed using ThermoFluor++ version 1.3.7 software to obtain melting temperature, T_m and extreme outliers were omitted.

Results and Discussion

1. Characterizing APT1 & 2 Mutants: Selectivity determinants

Individual contributions. I would first like to acknowledge and thank the members of the Martin Lab who have made significant contributions towards this portion of my thesis project. Although I helped purify some of the enzymes used, Christina Rodriguez, Laura Rodriguez and Michael Won performed most of the bacterial transformations and protein purifications to obtain WT and mutant APTs for study. Michael Won and Dr. Dahvid Davda provided much advice and direction for this project, and aided with the data analysis and generation of figures. Dr Dahvid Davda also worked on obtaining the crystal structures of APT1 and APT2 and generating figures for this thesis. Primarily, my principal investigator, Dr. Brent Martin, conceived the main idea for this project, provided funding and gave direction on the experiments that were conducted. My role was to optimize the conditions for the assays, perform the substrate-dependence and dose-response assays, perform initial analysis of the data, and write up this chapter.

Background. In order to elucidate the mechanism behind the substrate specificity of APT1 and APT2, other members in our lab have previously crystallized and obtained the structures of APT1 and APT2 bound to their isoform specific inhibitors, ML348 and ML349 respectively. Upon examining the protein-inhibitor interactions in the resulting protein structures, it was observed that several highly conserved residues that were located in homologous positions in both proteins were different between APT1 and APT2. These residues appeared to interact differently with ML348 and ML349, and were thus hypothesized to contribute to inhibitor specificity. These residue pairs are as follow: I75^{APT1}/L78^{APT2}, Q83^{APT1}/P86^{APT2}, R149^{APT1}/H152^{APT2} and L176^{APT1}/M178^{APT2}.

In order to test this hypothesis, mutant forms of APT1 and 2 were made such that the homologous residues described above were switched between the two isoforms and

tested for substrate selectivity using ML348 (APT1-WT selective) and ML349 (APT2-WT selective). Several orthogonal methods were used to confirm our hypothesis, including drug target residency time assays, but within the context of this thesis I will only discuss the results of the two assays which I was involved in: the steady state hydrolysis of the ResOAc substrate analog assay and the thermal stability assay.

Results & Discussion. We first assayed the steady-state rate of hydrolysis of ResOAc by WT and mutant APT1 and 2 in order to ensure that the point mutations did not significantly alter the activities of the enzyme. As shown in Figures 5B and C below, all the mutants did not show significantly different K_m values towards ResOAc as compared to WT. This is important, as K_m values of the enzymes will be used in later calculations to determine the affinity of the enzymes towards inhibitors¹⁵, K_i , and we want to ensure that any observed difference in K_i values is due to different enzyme-inhibitor interactions, and not altered enzyme-substrate interactions.

No significant difference was observed in V_{max} and k_{cat} among APT1-WT and its mutants, but surprisingly V_{max} and k_{cat} values were about 4 fold higher in all of the APT2 mutants compared to the WT. This may indicate that APT2 mutants are more efficient at turning over ResOAc or clearing the active site once the reaction is complete. Nevertheless, since V_{max} and k_{cat} are not involved in calculating the K_i of inhibitors, this result will not influence our later experiments.

Inhibitor dose-dependence experiments were then performed on all the APT1 and 2 WT and mutant enzymes against ML348 (APT1-selective) and ML349 (APT2-selective) and IC_{50} and K_i values were calculated from the data shown in Figure 5B-G.

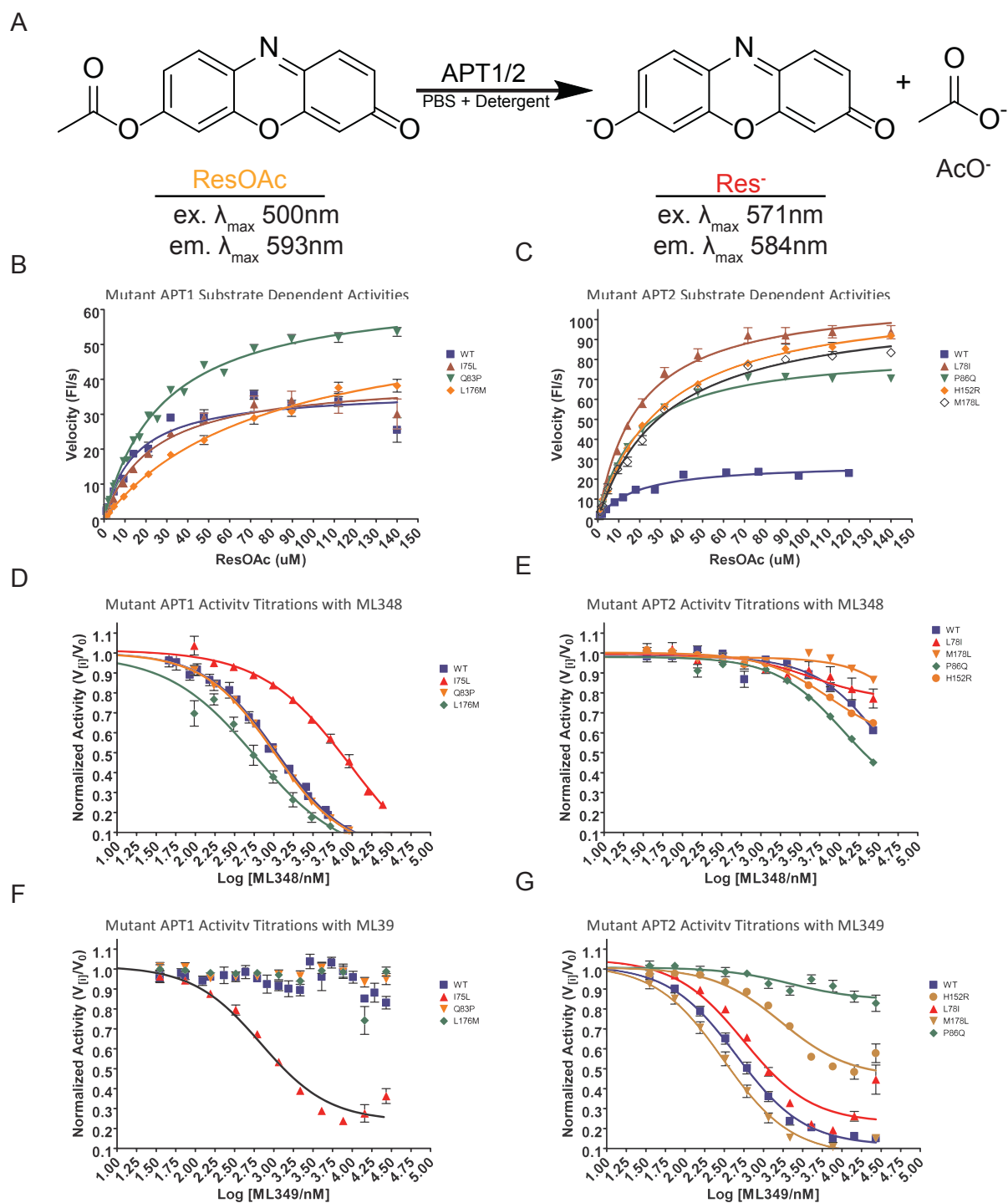


Figure 5: Results of the kinetic characterization of APT1 & 2 WT and mutant enzymes with the ResOAc substrate analog. (A) Fluorescent ResOAc was used as a substrate analog to assay the affinities of WT and mutant APT1 & 2 for ML348 and ML349. (B) & (C): Substrate-dependence of APT1-WT and its mutants, and APT2-WT and its mutants respectively against ResOAc. (D) & (E) Dose-dependent inhibition curves of ML348 towards APT1 and its mutants, and APT2 and its mutants respectively. (F) & (G) Dose-dependent inhibition of ML349 towards APT1 and its mutants, and APT2 and its mutants respectively.

Among the APT1 point mutants assayed, only the I75L substitution showed reversion to APT2-like behavior as it lost considerable affinity for ML348 (~10 fold decrease in K_i), as seen in Figure 5D, but gained sensitivity towards ML349 ($K_i = 218$ nM) close to that observed in APT2-WT, as shown in Figure 5E.

As for the APT2 point mutants, only the P86Q substitution gained any detectable affinity towards ML348 ($K_i = 3090$ nM), and even then its affinity is 10 fold higher than that of APT1 wild type, as seen in Figure 5F. However, two of the APT2 mutants, P86Q and H152R, drastically lost affinity for ML349, with the P86Q mutant being completely unable to bind ML349, as shown in Figure 5G. These numerical results are tabulated in Table 1 below.

Interestingly, though APT1-I75L showed reversion, APT2-L51I did not. The same was observed with the APT2-P86Q reversion, and the APT1-Q83P, which did not revert. This implies that perhaps more than one residue is involved in coordinating ligand specificity in the active site.

Enzyme	ResOAc K_m (μ M)	ResOAc V_{max} (FI/s)	ML348 K_i (nM)	ML349 K_i (nM)
APT1	14.99 \pm 2.075	37.01 \pm 1.399	300	>30
APT1-I75L	23.33 \pm 3.676	40.41 \pm 2.022	3147	218
APT1-Q83P	27.81 \pm 1.274	65.93 \pm 1.016	361	>30
APT1-L176M	76.94 \pm 8.408	60.09 \pm 3.245	354	>30
APT2	17.91 \pm 2.562	27.90 \pm 1.220	>30	230
APT2-L78I	19.35 \pm 1.392	111.9 \pm 2.396	>30	156
APT2-P86Q	18.71 \pm 0.651	84.72 \pm 0.873	3090	>30
APT2-M178L	32.35 \pm 1.739	106.6 \pm 2.046	>30	122
APT2-H152R	30.48 \pm 1.211	111.6 \pm 1.550	2930	5350

Table 1. Summary of the K_m and V_{max} of the APT1 and 2 enzymes and their point mutants, along with their K_i values towards ML348 and ML349.

In order to validate the kinetic results observed with the APT1-I75L and APT2-P86Q, we performed thermal stability measurements to determine the melting temperature, T_m of the wild type and mutant enzymes.

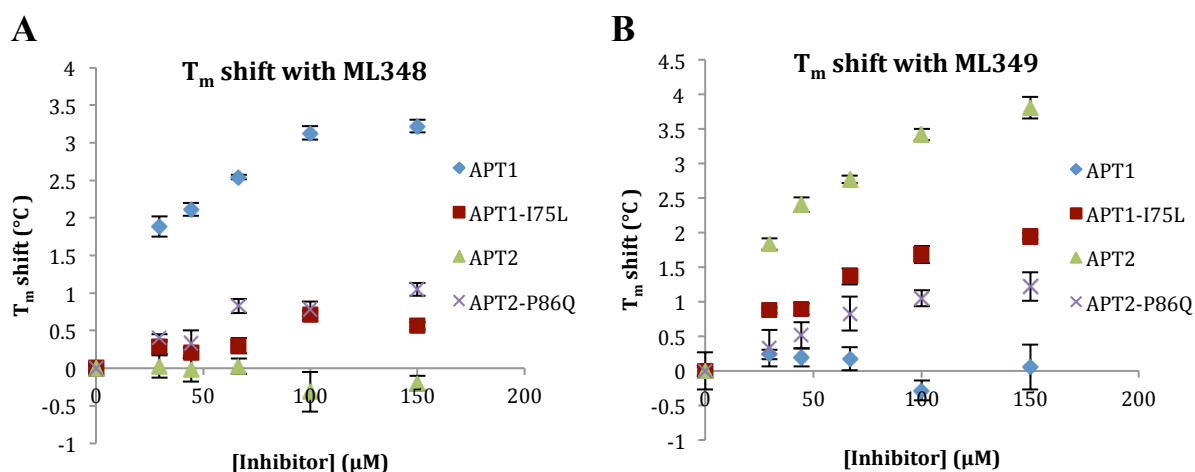


Figure 6: Results of the thermal shift assays characterizing the T_m of APT1, APT1-I75L, APT2 and APT2-P86Q when (A) preincubated with ML348 or when (B) preincubated with ML349.

The thermal shift assay supports our previous findings that APT1-I75L and APT2-P86Q show inversion of selectivity. Both APT1-I75L and APT2-P86Q display intermediate T_m phenotypes between APT1 and APT2 when bound with either ML348 or ML349 as shown in Figure 6A and B. This suggests that with APT1, the I75L mutation reduces thermal stabilization with ML348, while promoting stabilizing interactions with ML349. At the same time, with APT2, the P86Q mutation promotes stabilizing interactions with ML348 while reducing thermal stabilization with ML349. However, the T_m shifts observed with both point mutants are not very large ($< 2^\circ\text{C}$), so it is difficult to make conclusions with strong confidence. There are likely other factors besides thermal stabilization that contributes to the inversion observed in the steady-state kinetic assays.

It is difficult to define how single point mutations can cause inversion in substrate selectivity of APT1 and APT2. Mapping the I75/L78 and Q83/P86 onto the structures of APT1 and APT2, we can see that these residues flank the lower active site-capping loop, as shown in Figure 6. The residues in this region probably affect the conformation dynamics of this loop, and possibly the accessibility of substrates or inhibitors into the active site. We hypothesize that perhaps the P86 and L78 residues on

APT2 together confer more rigidity to the active site-capping loop. As ML348 is predicted to have more rotational degrees of freedom than ML349 due to its greater number of freely rotating bonds, perhaps the binding of ML348 to a more rigid active site as hypothesized in APT2 would be disfavored due to entropic reasons. Nevertheless, more studies need to be done to validate this hypothesis.

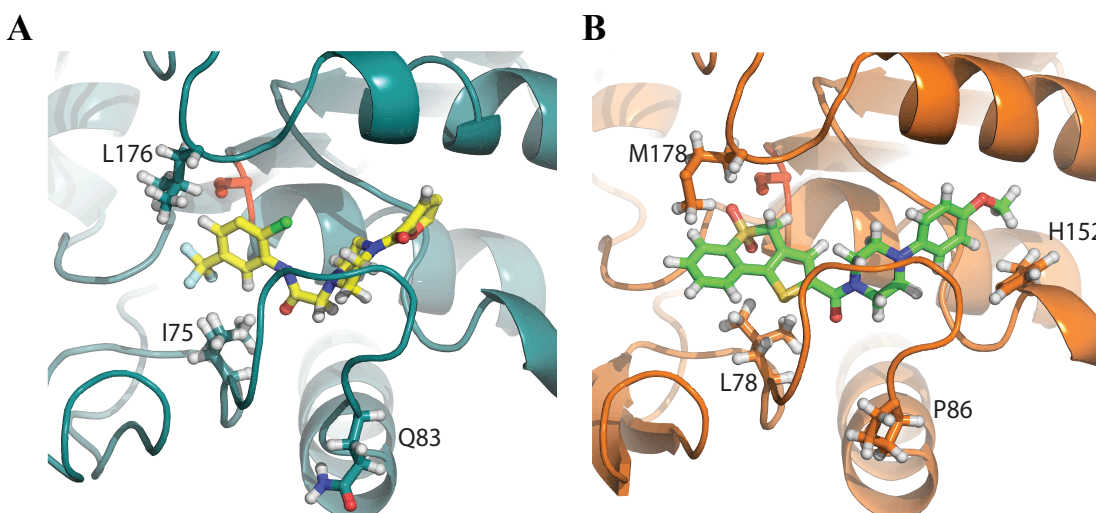


Figure 7: Depiction of the active site of APT1 and APT2 along with their isoform-specific inhibitors docked in the active site. Residues that were mutated are shown in stick representations and labeled. (A) ML348 docked in the active site of APT1. (B) ML349 docked in the active site of APT2

2. Characterizing ML349 inhibitor derivatives: What defines the active site?

Individual contributions. As described before, I am thankful to Christina Rodriguez, Laura Rodriguez and Michael Won who performed most of the bacterial transformations and protein purifications to obtain WT and mutant APTs for study. Dr. Jaimeen Majmudar, Michael Won and Andrea Chong synthesized the various ML349 derivatives that were probed. Michael Won and Dr. Dahvid Davda provided much advice and direction for this project, and Dr. Dahvid Davda aided significantly with the data analysis and generation of figures. Primarily, my principal investigator, Dr. Brent Martin, conceived the main idea for this project, provided funding and gave direction on the experiments that were conducted. My role was to optimize the conditions for the

assays, perform dose-response assays and thermal stability assays, perform initial analysis of the data, and write up this chapter.

Background. In addition to probing residues that determine specificity of the active site, we wanted to further characterize the steric and electronic requirements for binding the active site of APT1 and APT2. One hypothesis derived from the crystal structure of APT2 with ML349 was that ML349 binding was partially due to its sulfone group (not found in ML348), which mimicked the tetrahedral intermediate of the transition state when associating with the catalytic serine hydroxyl. To test this, we synthesized two ML349 derivatives with increasingly reduced groups on the sulfone moiety, termed ML349-sulfoxide and ML349-thioether. The reasoning behind this is that if the oxygen atoms of the sulfone moiety were critical in hydrogen bonding with the catalytic serine to mimic the transition state, then removal of those oxygen atoms should abrogate binding of ML349 to APT2.

Further, if formation of a tetrahedral intermediate-like structure plays a key role in the binding of ML349 to APT2, then a catalytically dead APT2-S122A in which the catalytic serine is mutated to an alanine that can no longer hydrogen bond should have show a reduced T_m shift compared to WT APT2 when bound to ML349. The contribution of the sulfone-catalytic serine interaction towards stabilizing ML349 binding to APT2 could not be assayed using the substrate-based hydrolysis of ResOAc as the S122A has no catalytic activity and cannot hydrolyze ResOAc. Thus, we plan to use the thermal stability assay to probe this interaction.

At the same time, we also wanted to characterize the binding of the opposite end of ML349, as the crystal structure of ML349 bound to the APT2 active site suggests that this region may lie in the hydrophobic channel in APT2 that dictates ligand specificity.

To test this, we synthesized various ML349 derivatives, referred to as the methoxy series, with the substitution of various groups of differing length, size and polarity. The full list of compounds tested, along with their K_i values for both APT1 and APT2 is included at the end of this section in Supplementary Figure 1.

Results and Discussion. We first used steady-state inhibitor dose-dependence assays to determine the contribution of the sulfone moiety to the binding of ML349 to APT2. Indeed, the removal of the first oxygen atom from the sulfone group increases the K_i of ML349 for APT2 drastically by almost 20 fold (105.30 nM for ML349, 2222.35 nM for ML349-sulfoxide). This suggests the critical importance of both oxygens at the sulfone moiety, as ML349-sulfoxide was added as a racemic mixture, and if only one of either oxygen atom would suffice, then the transition from sulfone to sulfoxide would only result in a small 2-3 fold increase in K_i , unlike the 20-fold increase observed. The removal of the second oxygen atom further increases the K_i of the ML349-thioether above the detectable level of our assay ($> 10,000$ nM), as shown in Figure 8 below, further iterating the importance of the sulfone moiety.

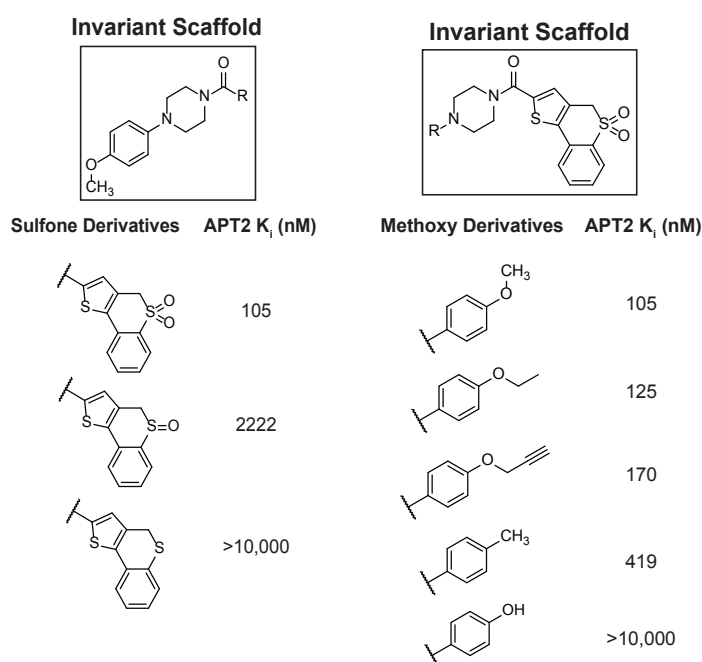


Figure 8: K_i values for ML349 derivatives of the sulfone moiety and the methoxy group. The compounds in the first row depict the sulfone and methoxy regions of the lead APT2 inhibitor, ML349.

The results of the thermal stability assay of APT2 with ML349 and the reduced thioether derivative support our results as the thioether derivative showed no significant thermal stabilization of APT2, as shown in Figure 9A below. Surprisingly, the APT2-S122A mutant, which lacks the catalytic serine hydroxyl group that putatively binds the ML349 sulfone, shows a comparable T_m shift when treated with ML349 compared to APT2-WT, as shown in Figure 9B below. This implies that ML349 is still able to form stabilizing interactions with APT2-S122A even without the sulfone-serine hydroxyl interactions. It might be that the stabilization of the sulfone group of ML349 is not only coordinated by the catalytic serine, but also other polar residues in that region, which would be thus be drastically abrogated should any of the sulfone oxygens be removed.

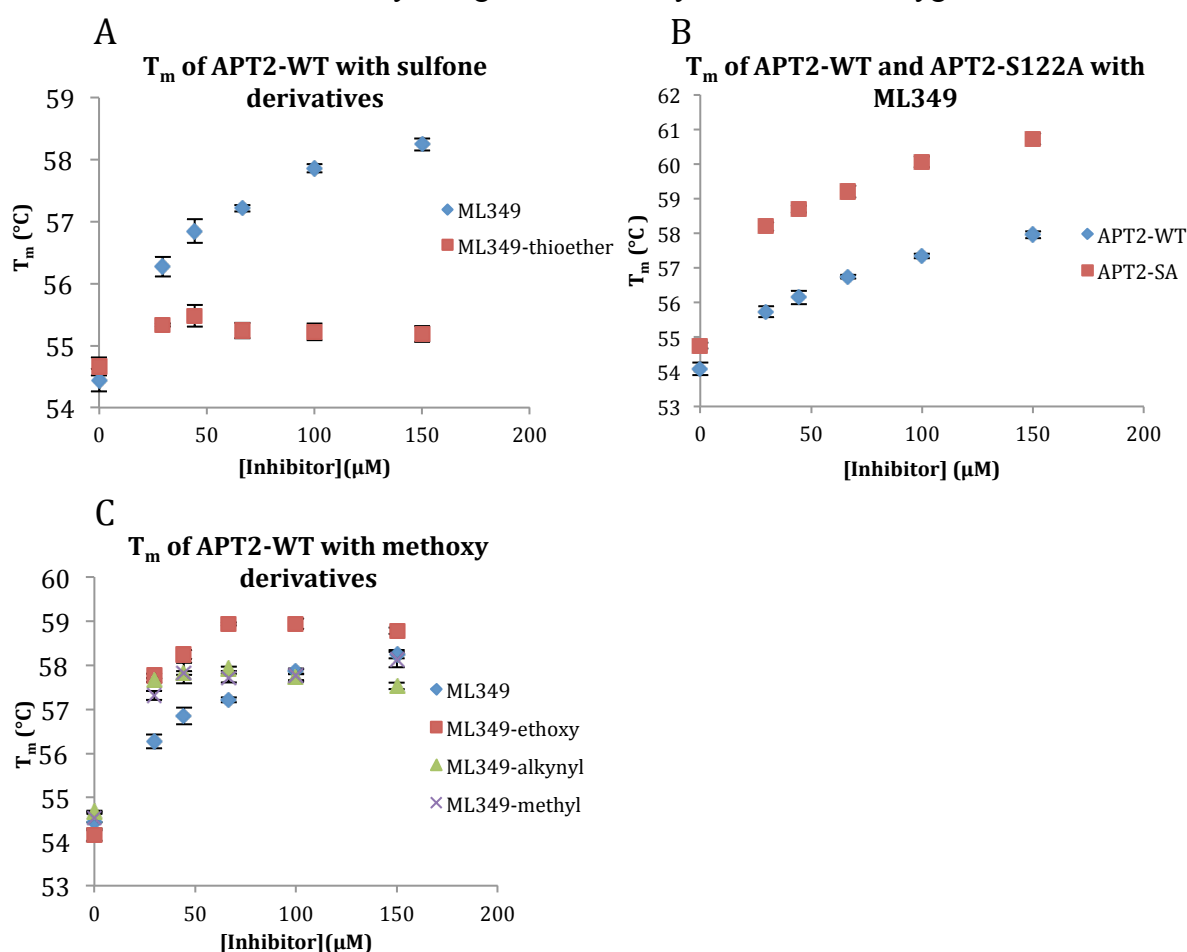


Figure 9: Thermal stabilization assay results for ML349 derivatives. (A) T_m of APT2-WT with ML349 and ML349-thioether. (B) T_m of APT2-WT and APT2-S122A against ML349. (C) T_m of APT2-WT against the ML349 methoxy derivatives.

We also used the inhibitor dose-dependence assays to obtain K_i values for the methoxy series of ML349 derivatives. Interestingly, when we compared the affinity of APT2 for derivatives with longer, aliphatic ethoxy or O-alkynyl substitutions with that for ML349, we don't see an appreciable difference in K_i values, as seen in Figure 8 above. On the other hand, when we substituted the methoxy group on ML349 with the shorter methyl and hydroxyl groups, we see that the affinity of APT2 for these compounds is much weakened. This suggests that perhaps APT2 favors long aliphatic substrates to facilitate interaction with its hydrophobic surfaces. When we compared this result to that obtained using the thermal stability assay, we observe that the T_m shifts of APT2 were not significantly different between the ethoxy, alkynyl, methyl and unaltered ML349, suggesting that the contribution of these groups towards the binding of APT2 is comparable to each other, as seen in Figure 9C.

Interestingly, the inhibitor dose-response assay showed that several compounds in the ML349 methoxy series also showed affinity for both APT1-WT and APT2-WT. These compounds include the alkynyl, acetyl and desmethoxy derivatives of ML349, and were termed ML349 dual inhibitors (Supplementary Figure1). However, when we assayed these compounds using the thermal stability assay against APT1-WT and

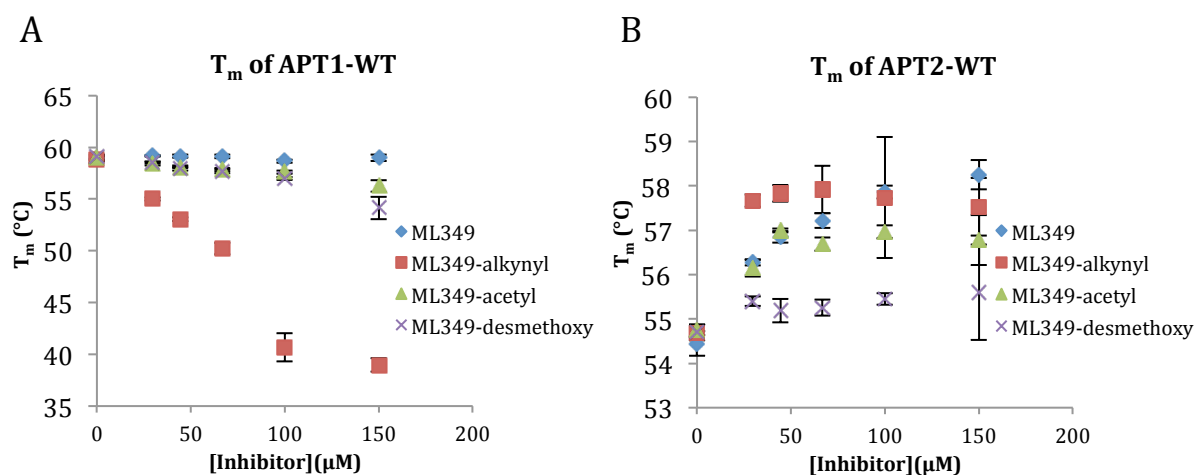
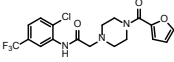
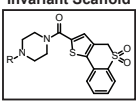
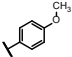
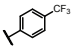
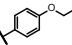
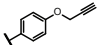
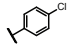
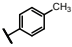
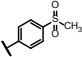
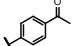
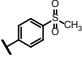
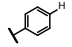
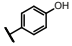
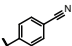
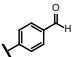
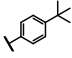
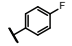
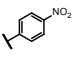
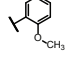


Figure 10: Thermal stabilization assay results for ML349 methoxy derivatives that inhibit both (A) APT1-WT and (B) APT2-WT

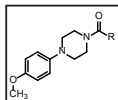
APT2-WT, the results suggest that the dual inhibitors affect both enzymes via different mechanisms. As seen in Figure 10A, the dual inhibitors have a destabilizing effect on APT1-WT, whereas Figure 10B shows that the same compounds have a stabilizing effect on APT2-WT. We hypothesize that in the case of APT1, the compound may be binding the active site in such a way that perturbs the tight packing of the enzyme, allowing solvent access to the protein core, thus destabilizing the enzyme. On the other hand, the stabilization of APT2 by the same compounds implies that inhibition is achieved by enthalpic stabilization of the protein-ligand complex by the compounds, thus competing with the substrate for access to the active site. However, this is just our initial hypothesis and further experiments need to be conducted to determine how the previously APT2 isoform-selective ML349 gained affinity for APT1 merely through substitutions in the methoxy group.

In summary, we have shown that the highly oxidized sulfone group of ML349 plays a critical role in selectively binding the active site of APT2, possibly through hydrogen bonding and the formation of a mimic of the transition state tetrahedral intermediate. We have also shown that the methoxy group of ML349 is likely a key determinant of its enzyme selectivity, as substitutions of this group can cause the compound to gain potency towards APT1. We also hypothesize that the long hydrophobic channel leading to the APT2 catalytic site may predispose APT2 towards longer, aliphatic substrates, due to the enzyme's affinity for ML349 with longer hydrophobic groups substituted at the methoxy position. However, further experiments using native substrates are necessary to further probe the active site of APT2. One future direction for this project would be to test the dose-dependence of APT1 and APT2 against fatty acids of different lengths and degrees of saturation in order to identify the possible native substrates of these enzymes.

Supplementary Figure 1: List of K_i values for ML348, ML349 as well as methoxy, sulfone, and biotinylated derivatives of ML349 against APT1, APT2 and APT1-I75L.

Type	Compound name	Structure	APT1 K_i (nM)	APT2 K_i (nM)	I75L.APT1 K_i (nM)
Lead APT1 Compound	ML348		250	>10,000	2233
		Invariant Scaffold 			
Lead APT2 Cmpnd	ML349		>10,000	105	290
Methoxy Derivative	AC-2-39		>10,000	28	N/A
Methoxy Derivative	AC-2-42		>10,000	125	1359
Methoxy Derivative	Alkyne-ML349		437	170	342
Methoxy Derivative	AC-2-46		4173	176	N/A
Methoxy Derivative	AC-2-40		>10,000	419	N/A
Methoxy Derivative	AC-2-37		1758	467	N/A
Methoxy Derivative	Ac-ML349		398	490	N/A
Methoxy Derivative	AC-2-38		>10,000	936	N/A
Methoxy Derivative	DesMe-ML349		261	1064	N/A
Methoxy Derivative	AC-2-41		>10,000	>10,000	N/A
Methoxy Derivative	AC-2-43		>10,000	>10,000	N/A
Methoxy Derivative	AC-2-44		5706	>10,000	N/A
Methoxy Derivative	AC-2-45		>10,000	>10,000	N/A
Methoxy Derivative	AC-2-47		>10,000	>10,000	N/A
Methoxy Derivative	AC-2-48		>10,000	>10,000	N/A
Methoxy Derivative	o-MeO-ML349		>10,000	>10,000	N/A

Invariant Scaffold



Sulfone Derivative	TB2		2346	260	N/A
Sulfone Derivative	SJS14		>10,000	1974	N/A
Sulfone Derivative	EH11b		>10,000	2222	N/A
Sulfone Derivative	TB1		>10,000	>10,000	N/A
Sulfone Derivative	TB3		>10,000	>10,000	N/A
Sulfone Derivative	EH22		>10,000	>10,000	N/A
Sulfone Derivative	SB1		3696	>10,000	N/A
Sulfone Derivative	SB2		>10,000	>10,000	N/A
Sulfone Derivative	SB22		5841	>10,000	N/A
Biotinylated ML349 Derivative	Thioether-ML349-PB		637	657	N/A
Biotinylated ML349 Derivative	ML349-PB		1971	765	N/A
Biotinylated ML349 Derivative	o-MeO-ML349-PB		810	>10,000	N/A
Biotinylated ML349 Derivative	N3-PB		>10,000	>10,000	N/A

Acknowledgements

Just four years ago, I would have never imagined myself being capable of getting involved in scientific research, let alone overcoming the daunting prospect of writing a thesis. Everything that I have accomplished here could not have been achieved without the invaluable support, encouragement and endless help that I have been so blessed to receive from the many individuals who have played significant roles in my undergraduate journey.

Firstly, praise and glory be to God through whom I have been blessed with the wonderful people who have guided me throughout this journey. He has opened doors to numerous opportunities, strengthened me to persevere through difficulties and given me so much grace and mercy when I messed up. Without his blessing and providence, I could never hope to succeed in this endeavor.

None of this would have been possible without the guidance of my faculty mentor and primary investigator, Dr. Brent R. Martin. He conceived the idea and direction behind this project and guided me throughout its execution and evolution into the results we see today. He has taught me so much about how science is done in the real world, and encouraged me and believed in me even when I did not believe in myself. Thank you for giving me this chance and opportunity.

I also owe countless thanks to Dr. Dahvid Davda and Michael Won for all the life-saving help they have given me. Thank you for always being patient with my endless questions, for teaching me how to patiently troubleshoot assays that just will not work, for wading through the messiness of imperfect data together with me, and always providing guidance and direction. I truly treasure your mentorship.

Thanks also go out to the other members of the Martin lab who have walked on this journey together with me. Thank you for helping me find Michael, Dahvid or Dr.

Brent when I needed their help, for helping me find or borrow the reagents I desperately need, and for showing me that researchers are lively, caring people, and not just zombies working 9 to 5. I am especially thankful for my fellow member of the Martin Lab, Andrea Chong, who is also my housemate. We have struggled through this journey together and I am thankful for all those nights at home stressing over poster presentations and thesis submissions together with you.

I also have to thank Priya Chinnaswamy from the Life Science Institute at the University of Michigan for teaching me how to conduct the thermal melting experiments and patiently walking me through all my questions and problems when they inevitably popped up.

I would also like to especially thank Dr. Shan Wan and Dr. Theodore Welling, who were my first research mentors and introduced me to the exciting field of medical research back when I was still a freshman with absolutely zero experience in a lab. I have learnt so much from my time with you, and it is truly thanks to you that I first fell in love with research.

I am also grateful to my brothers and sisters in Harvest Mission Community Church who have supported me emotionally and spiritually throughout this harrowing journey. Thank you for all your prayers and encouragement.

Last but not least, I owe everything to the love and support of my mum, dad and little brother. Thank you for your unconditional love that inspires me to give my all to everything I do. Thank you for raising me to be the person I am today. Thank you for encouraging me and helping me find the silver lining. And most of all, thank you for listening to all my science rants and feigning interest in what I do, even when I likely didn't make much sense.

References

1. Agudo-Ibáñez L, Herrero A, Barbacid M, Crespo P. H-ras distribution and signaling in plasma membrane microdomains are regulated by acylation and deacylation events. *Mol Cell Biol.* 2015;35(11):1898-1914. doi:10.1128/MCB.01398-14.
2. Goodwin JS, Drake KR, Rogers C, et al. Depalmitoylated Ras traffics to and from the Golgi complex via a nonvesicular pathway. *J Cell Biol.* 2005;170(2):261-272. doi:10.1083/jcb.200502063.
3. Adibekian A, Martin BR, Chang JW, et al. Confirming target engagement for reversible inhibitors in vivo by kinetically tuned activity-based probes. *J Am Chem Soc.* 2012;134(25):10345-10348. doi:10.1021/ja303400u.
4. Davda D, Martin BR. Acyl protein thioesterase inhibitors as probes of dynamic S-palmitoylation. *Medchemcomm.* 2014;5(3):268-276. doi:10.1039/C3MD00333G.
5. Yeste-Velasco M, Linder ME, Lu YJ. Protein S-palmitoylation and cancer. *Biochim Biophys Acta - Rev Cancer.* 2015;1856(1):107-120. doi:10.1016/j.bbcan.2015.06.004.
6. Mitchell DA, Mitchell G, Ling Y, Budde C, Deschenes RJ. Mutational analysis of *Saccharomyces cerevisiae* Erf2 reveals a two-step reaction mechanism for protein palmitoylation by DHHC enzymes. *J Biol Chem.* 2010;285(49):38104-38114. doi:10.1074/jbc.M110.169102.
7. Fukata Y, Iwanaga T, Fukata M. Systematic screening for palmitoyl transferase activity of the DHHC protein family in mammalian cells. *Methods.* 2006;40(2):177-182. doi:10.1016/j.ymeth.2006.05.015.
8. Sugimoto H, Hayashi H, Yamashita S. Purification, cDNA cloning, and regulation of lysophospholipase from rat liver. *J Biol Chem.* 1996;271(13):7705-

7711. doi:10.1074/jbc.271.13.7705.
9. Duncan JA, Gilman AG. A cytoplasmic acyl-protein thioesterase that removes palmitate from G protein ?? subunits and p21(RAS). *J Biol Chem.* 1998;273(25):15830-15837. doi:10.1074/jbc.273.25.15830.
 10. Devedjiev Y, Dauter Z, Kuznetsov SR, Jones TLZ, Derewenda ZS. Crystal structure of the human acyl protein thioesterase I from a single X-ray data set to 1.5 ?? *Structure.* 2000;8(11):1137-1146. doi:10.1016/S0969-2126(00)00529-3.
 11. Hernandez JL, Majmudar JD, Martin BR. Profiling and inhibiting reversible palmitoylation. *Curr Opin Chem Biol.* 2013;17(1):20-26. doi:10.1016/j.cbpa.2012.11.023.
 12. Kang R, Wan J, Arstikaitis P, et al. Neural palmitoyl-proteomics reveals dynamic synaptic palmitoylation. *Nature.* 2008;456(7224):904-909. doi:10.1038/nature07605.
 13. Tomatis VM, Trenchi A, Gomez GA, Daniotti JL. Acyl-protein thioesterase 2 catalyzes the deacylation of peripheral membrane-associated GAP-43. *PLoS One.* 2010;5(11). doi:10.1371/journal.pone.0015045.
 14. Tian L, McClafferty H, Knaus HG, Ruth P, Shipston MJ. Distinct acyl protein transferases and thioesterases control surface expression of calcium-activated potassium channels. *J Biol Chem.* 2012;287(18):14718-14725. doi:10.1074/jbc.M111.335547.
 15. Yung-Chi C, Prusoff WH. Relationship between the inhibition constant (KI) and the concentration of inhibitor which causes 50 per cent inhibition (I50) of an enzymatic reaction. *Biochem Pharmacol.* 1973;22(23):3099-3108. doi:10.1016/0006-2952(73)90196-2.